Modeling the Displacement in Three-Layer Electroactive Polymers Using Different Counter-Ions by a Phase Transformation Approach

J. F. Guzman,[1,2] J. A. Cortes,[1] A. Fuentes,[1] T. Kobayashi,[2] Y. Hoshina[2]

[1]*Centro de Innovacion en Diseño y Tecnologia, Instituto Tecnologico y de Estudios Superiores de Monterrey (ITESM) Campus Monterrey. Ave. Eugenio Garza Sada 2501 Sur, Col. Tecnologico, 64849 Monterrey, NL, Mexico*
[2]*Department of Chemistry, Nagaoka University of Techonology, Nagaoka, Niigata 9402188, Japan*

Received 3 June 2008; accepted 2 November 2008
DOI 10.1002/app.29684
Published online 4 March 2009 in Wiley InterScience (www.interscience.wiley.com).

ABSTRACT: The use of three-layer electroactives polymers is becoming more widely known among researchers and engineers because of their potentials to become mechanical actuators. The up-to-date research and development in the Nafion®/Metal composites has given some fundamentals, preparation techniques, and modeling of the phenomena regarding the deformation of the material from different scientific point of view. This gives the opportunity to propose correlations for modeling the phenomena present in these materials by different approaches. A constitutive model for the bending deformation of a Nafion® Ionic Polymer-Metal Composite (IPMC) was formulated based on an approach that represents, analogically, a phase transformation inside the base polymer and combines it with the bending of a beam in order to predict the displacement when the material is subject to an electrical input. The model was solved and evaluated for five different types of counter-ion systems. Experimental data was used to solve the parameters within the model. The results of the solved model gave a good fitting of the experimental data and are shown for different voltage and frequency conditions in all five ionic systems. © 2009 Wiley Periodicals, Inc. J Appl Polym Sci 112: 3284–3293, 2009

Key words: electroactive polymer; composite; modeling; membranes; polyelectrolytes

INTRODUCTION

Electroactives polymers are functional materials that have grasped the attention of researchers and engineers in the recent years. Ionic Polymer-Metal Composites (IPMC) are electroactive polymers that consist in three-layer arrangements between an ion-exchange resin and a set of metal electrodes built on the polymer surface through chemical reactions. These materials are able to exhibit large deformations when placed in a time varying electric field.[1–3] Although scientists have been working with electroactive polymers, several of the phenomena associated to the IPMC are still under active research. It is observed that, in general, the phenomena associated to the bending are still in ways to be explained in engineering standards for practical interpretation, design and application. In the meanwhile, different approaches to model the particular features found in IPMC are possible. The up-to-date research and development in the IPMC as actuators or sensors has given some fundamentals, preparation techniques, and modeling of the phenomena regarding the deformation of the material from a scientific point of view.[4–7]

To name some examples, considering only the report advances as from the year 2000,[8] de Gennes, Okumura, Shahinpoor, and Kim and coworkers[9] presented the first phenomenological theory for sensing and actuation in IPMC based on linear irreversible thermodynamics, with two driving forces (E and a water pressure gradient ∇p) and two fluxes (electric current and water current). Asaka and Oguro[10] discussed the bending of polyelectrolyte membrane-platinum composites by electric stimuli and presented a theory on actuation mechanisms in IPMC by considering the electro-osmotic drag term in transport equations. Nemat-Nasser and Li[11] presented a modeling on the electromechanical response of ionic polymer-metal composites based on electrostatic attraction/repulsion forces in the IPMC. Later, Nemat-Nasser[12] presented a revised version of their earlier article and stressed the role of hydrated cation transport within the clusters and polymeric networks in IPMC. Nemat-Nasser and Wu[13] have presented a discussion on the role of back bone ionic polymer and in particular sulfonic versus carboxylic ionic polymers, and the effect of different cations such as K^+, Na^+, Li^+, Cs^+, and some organometalic cations on the actuation and

Correspondence to: J. F. Guzman (naisor@gmail.com).

sensing performance of IPMC's. Tadokoro,[14] Tadokoro et al.[15,16] have presented an actuator model of IPMC for robotic applications on the basis of physic-chemical phenomena.

All these different approaches found in the formulation of the mathematical aspects which try to explain such a particular feature (the bending action) found in IPMC materials, somehow had made many engineers to choose for actual experimentation (rather than one faithful approach) to have a basic understanding of the electroactive phenomenon to use it for specific design purposes; which consumes time and is still far to contribute to the establishment of standards in the field of giving applications to the material. In this work, an empirical model for the bending action of an IPMC strip was established using a phase transformation approach. It began with the formulation of the equations needed to describe the external and internal behaviors present in a strip of IPMC placed in a cantilever arrangement. The deformation of a beam is used to establish the external behavior of the polymer when subject to electrical stimulation. After this, the internal behavior of the counter-ions and water molecules is treat similar to a case of phase transformation such in the case of certain metals (where more than one physical phase coexist with the materials) with a suitable equation. This model, constructed from the external and internal behaviors of the electroactive polymers, uses parameters which are solved from experimental data obtained from an evaluation of displacement using different cation systems which achieve different degrees of deformation.

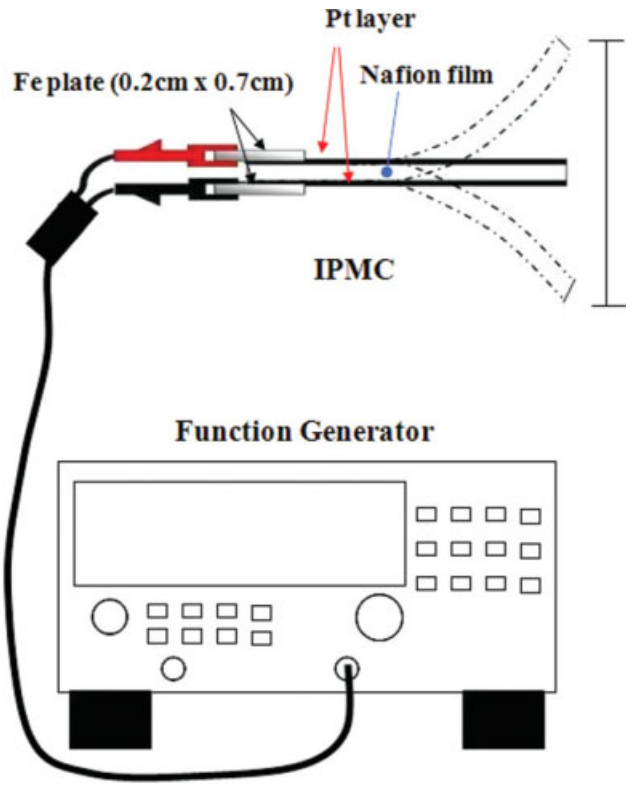

Figure 1 Diagram showing the proposed experimental setting for measuring the total displacement of an IPMC strip. [Color figure can be viewed in the online issue, which is available at www.interscience.wiley.com.]

EXPERIMENTAL

Materials

The IPMC films used were made by coating a Nafion® ion-exchange membrane with platinum in a series of oxidation and reduction reactions, according to Oguro et al.[1] Nafion® 117 was acquired from FuelCellStore (San Diego, CA). The Platinum complex salt, Tetraamineplatinum(II) Chloride, and other reactants were purchased from Sigma-Aldrich (St. Louis, MO). IPMC strips (1.0×3.0 cm^2) samples with deposited metallic layers made of Platinum were specially treated to have mainly Lithium (Li^+), Potassium (K^+), Sodium (Na^+), Magnesium (Mg^{2+}), and Calcium (Ca^{2+}) counter-ions, respectively to be use in individual experiments to obtain displacement measurements.

Displacement evaluation

The design of the experimental setting is resumed as follows: for the electrical input, a function generator was used to provide stable electrical signal conditions by means of adjusting the voltage and frequency as required. To have a voltage over the IPMC, the strip was arranged in such a way that: (1) both electrodes are connected to the circuit, (2) the IPMC is fixed in a cantilever configuration, and (3) it is easy to measure the displacement at each experimental run. Figure 1 shows a diagram of the proposed experimental setting for the displacement evaluation.

The experiment for electroactive deformation is done using a FG-281 function generator (Kenwood TMI, Japan) to provide a square signal at controlled conditions of voltage and frequency. The output electrodes are fixed as Fe plates coated with gold and using a clamp to grab the IPMC sample in a cantilever arrangement. The Fe plate ends (0.2×0.7 cm^2) are connected with an RG-58A BCN Cable (Miyazaki, Japan) to observe the maximum displacement achieve at the tip of the free end of the polymer (Fig. 1). The deformation measurements are performed with the aid of a millimetric paper set in a carefully fixed perpendicular surface to achieve an accurate measure without interfering with the polymer's movement.

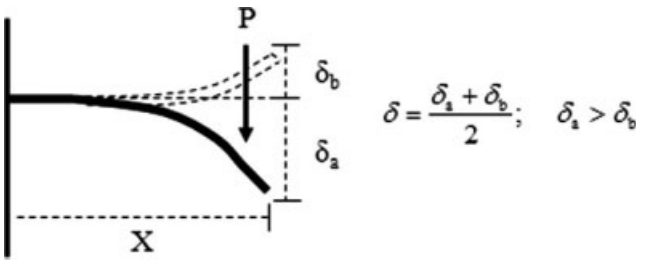

Figure 2 A system having a beam being deformed by a load (virtual) P, producing a total displacement δ.

Modeling of the displacement as a deforming beam

The modeling begins with the characterization of the system to be analyzed in its external behavior. The configuration of the IPMC is the same as a beam in a cantilever state, having one end fixed and the other end free for movement. When a load is applied to the system, a reversible deformation is produced. Where P is the load (virtual) responsible for the movement and δ is the maximum displacement obtained from the deformation; taking in account the existence of a reciprocal deformation when the system enters relaxation after the load disappears.

The deformation of the system may be expressed mathematically as a function of the load and the material properties along the length of the beam. By Hooke's law, it is known that the deformation over a beam system as presented in Figure 2 is given by:

$$\varepsilon(\chi) = \frac{\sigma(\chi)}{E} = \frac{PX}{EZ} \tag{1}$$

where σ(χ) is the bending stress on a beam or strip at a distance X from the point of application of the load to its fixed end. E is the modulus of elasticity of the material which composed the beam. Z is the section modulus, which is constant while the geometric shape does not change.

In this case, there is not a load P responsible for the displacement δ. However, this load exists as a respond to the potential difference given by an electric field. For this reason it is referred to as a virtual load. On the other hand, it is known that the displacement δ is directly proportional to this virtual load P, as shown in Figure 3. This is:

$$P = a \cdot \delta \tag{2}$$

where a in eq. (2) is a proportionality constant in mass/distance dimensions. Then eq. (1) may be written as:

$$\varepsilon = \left(\frac{aX}{ZE}\right)\delta$$

or

$$\delta = \left(\frac{ZE}{aX}\right)\varepsilon \tag{3}$$

where K is equal to:

$$K = \frac{ZE}{aX} \tag{4}$$

It is observed here that a and E are parameters that depend on the material. Also X and Z depend on the geometry and the position of the material. In eq. (3) the K is called a factor for the virtual, geometric, and material conditions. At normal conditions, a and E are constant as the material does not change its properties. In this case, however, the material will change its composition properties at the diffusion zones, and thus a and E will also change. Nevertheless, to begin the modeling it is considered that these parameters will remain constant.

Determining the factor K for the effect of the presence of the ion

After establishing the principles for the external behavior for the bending beam system, the following states regarding the internal changes within the material are considered, as shown in Figure 4.

The diffusion of particles (primarily cations and waters molecules) from a state A to B promotes the volumetric expansion in one side of the cross section of the thickness; and, thus, a volumetric contraction at the other side. In a particular region at a state A′, a lower concentration of the counter-ion is observed. After the migration it is possible to see that a larger

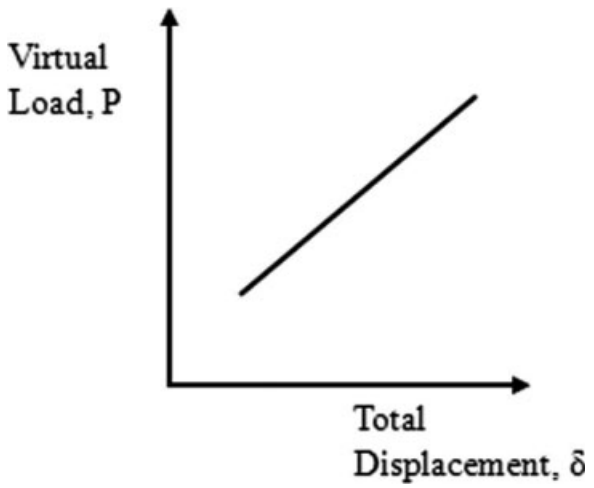

Figure 3 Linear relationship between the virtual load P and the total displacement δ.

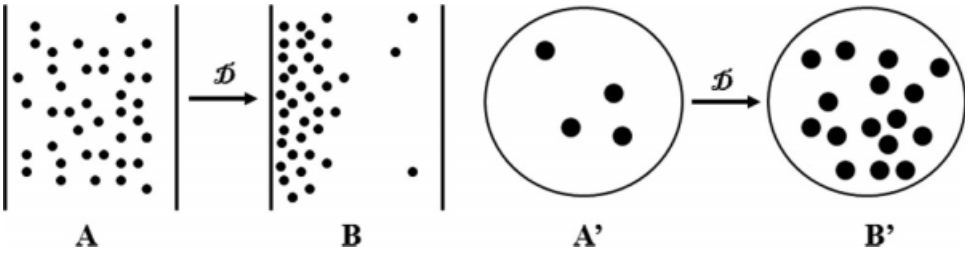

Figure 4 Diagram showing the change in the phase at one side of the cross section if the membrane. Where *D* is the Diffusion of cations from one side of the cross section to the other.

volume of particles or counter-ions in the same region or space previously at state A′ has allocated there, which turned into a state B′. This change let us relate the diffusive process as a phase transformation induced by an external factor, more than by transport phenomena. Since one of the sides will have a larger concentration than the other, A′ and B′ may be consider two phases coexisting at the same time in the material. It is proposed by this that the change in the physical-chemical state due to ion transport diffusion as a consequence of the application of a potential difference in an ionic polymer-metal composite, IPMC, is considered as a type of phase transformation in the material, induced by said potential difference. That way, the following behavior regarding the ionic migration within the polymeric cross section, while increasing the potential to diffuse by means of a voltage (*V*), should be seen, as shown in Figure 5.

Where, V_{f_i} is the volumetric fraction of the counter-ion present or missing in the material. The volumetric fraction is expressed by the next equation:

$$V_{f_i} = \frac{V_i}{V_T} \tag{5}$$

having,

$$1 \geq V_{f_i} \geq 0$$

where, V_i is the volume occupied by the counter-ion inside the polymer and V_T is the total volume in the material.

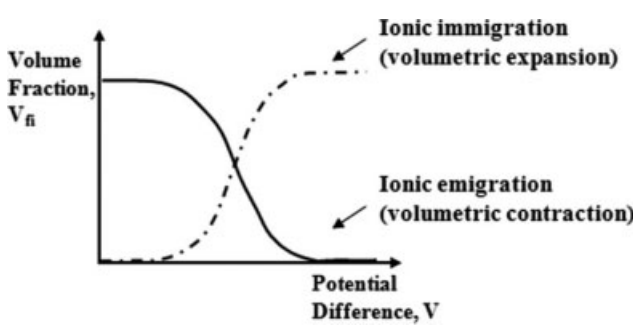

Figure 5 Behavior of the volume fraction at both side of the cross section of the membrane.

As most of the attention is toward the surface that expands, where the most of the counter-ions migrate, and because of the reciprocity of the phenomenon, it is possible to just consider the surface that expands. This way, by constant frequency (v) conditions and the migration of a certain size of counter-ion specie, V_{f_i} should be able to show the following behavior shown in Figure 6.

So, at the end, for other values of frequency conditions, the following behavior is obtained as seen in Figure 7.

To calculate the different curves of V_{f_i} within different voltages and frequency conditions, the model of phase transformation developed by Cortes and coworkers[18–21] may be analogically applied for these conditions in such a way that the following equation is obtained:

$$V_{f_i} = \left[1 + \left(\frac{V}{V_C}\right)^{-B}\right]^{-1} \tag{6}$$

where V is the potential difference in Volts, V_C is a characteristic potential difference at specific frequency conditions, and B represents a factor for the constitution of the material system (i.e., Nafion® with Lithium cations inside). Graphically, V_C represents the potential difference at 50% of transformation. This is explained graphically in Figure 8.

Then, it may be proposed that V_C and B are found in terms of the frequency (v) and the distinctive

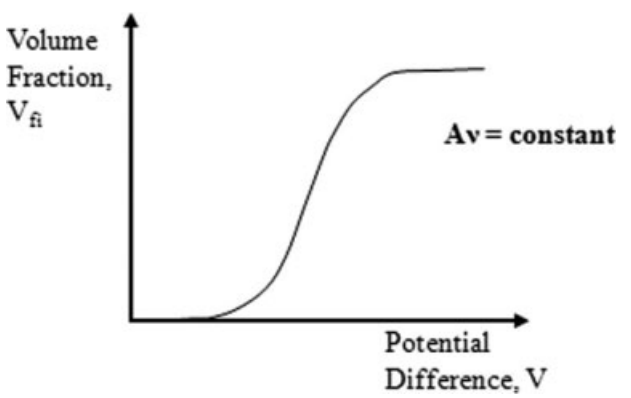

Figure 6 Behavior of the volume fraction V_{f_i} at the expanding side of the cross section at a specific frequency v.

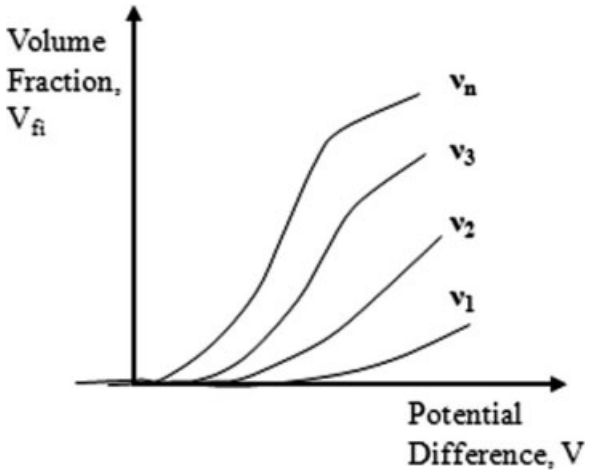

Figure 7 Behavior of the volume fraction V_{f_i} at the expanding side of the cross section at several frequency conditions.

characteristic of the embedded counter-ion, like the ionic radius (r_{ion}), respectively. This is:

$$V_C = fn(\nu); \quad B = fn(r_{\text{ion}}) \tag{7}$$

which is graphically shown in Figure 9. By substituting eq. (7) into eq. (6), there is

$$V_{f_i} = \left[1 + \left(\frac{V}{fn(\nu)}\right)^{-fn(r_{\text{ion}})}\right]^{-1} \tag{8}$$

The eq. (8) represents the volumetric fraction of the new transformed ionic phase. This means that it represents the volume fraction of the immigrated ions by the effect of the potential difference applied to the IPMC and the type of counter-ion being transported. However, for the results of this work, these were left as two parameters instead of functions in order to be solved as such and evaluate their tendencies through the change in frequency and ionic radius values correspondingly.

Retaking eq. (3), and emphasizing in the displacement of the strip in terms of the determination over the surface generated by the virtual load, and which it may be justified to be equal to the increase in the volume provided by the diffusion of the ionic phase in the surface of the strip, the total displacement of the previous external beam system may be expressed as:

$$\delta = K\varepsilon \tag{9}$$

as seen in Figure 10, for constant conditions of geometry and material properties.

When the material changes, the following behavior may be expressed graphically as in Figure 11.

Where the change in the material, in terms of the of the volume fraction of the contained ion specie, is observed as a particular composition of the achieved configuration.

This way, each slope is a particular function of the type of material under constant geometric conditions. Thus, as shown in Figure 12:

$$K = mV_{f_i} \tag{10}$$

where m is a proportionality constant. And so, eq. (10) is specify as:

$$K = m \cdot fn(\nu, r_{\text{ion}}) \tag{11}$$

Substituting eq. (8) in eq. (11), it results:

$$K = m \cdot \left[1 + \left(\frac{V}{fn(\nu)}\right)^{-fn(r_{\text{ion}})}\right]^{-1} \tag{12}$$

Which is the factor needed for eq. (3). It may be noticed that the factor K in eq. (12) is a function of the potential difference, the frequency, and the ionic characteristic. Also the proportionality constant m and the volume fraction of the ion play a role in the equations.

Equation (12) helps confirm that the factor K is parameter strongly dependant on the material properties and the operational conditions; so that it becomes a critical parameter that enables to distinguish the material under the mechanical effect of deformation-displacement of the same. However, as V_C and B in eq. (6) still do not have a physical meaning, they are considered here just as two values that vary with frequency and ionic radius respectively.

Determining the deformation as a function of the operational conditions

Parting from eq. (3) and substituting in eq. (12), it is given that

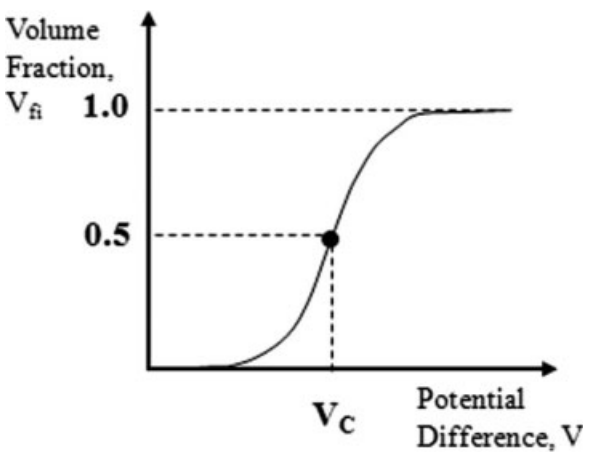

Figure 8 The characteristic voltage V_C is the value of potential difference at which the system is at 50% of transformation.

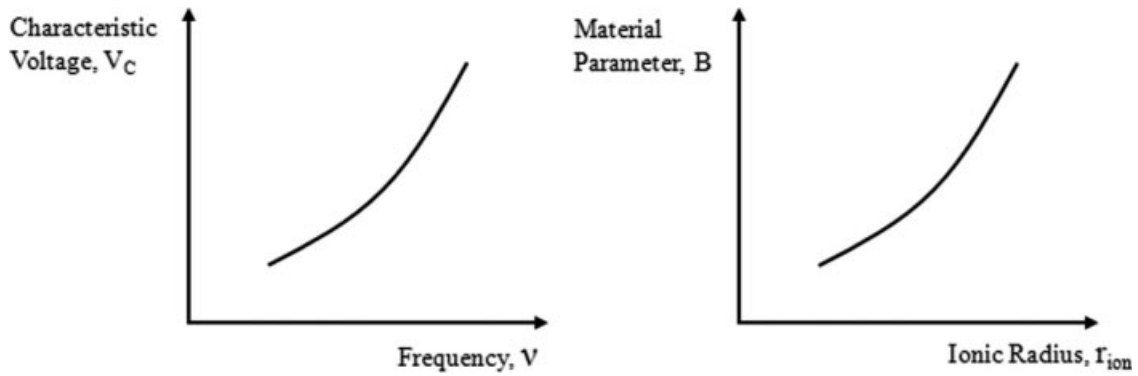

Figure 9 The possible behaviors of characteristic voltage V_C versus Frequency and the material parameter B versus the ionic radius.

$$\delta = m \cdot \varepsilon \cdot \left[1 + \left(\frac{V}{V_C}\right)^{-B}\right]^{-1} \tag{14}$$

Considering the deformation over a section of the surface as a variable with a very small magnitude and practically constant for the displacements obtained experimentally, it may be established that:

$$\alpha = m \cdot \varepsilon = \text{constant}$$

where,

$$\delta = \alpha \cdot \left[1 + \left(\frac{V}{V_C}\right)^{-B}\right]^{-1} \tag{15}$$

Equation (15) represents the constitutive model that let us predict the total displacement from the bending deformation action in the IPMC strip. To use this constitutive model, the three parameters, α, V_C, and B must be solved; which is the purpose of the steps to follow in the methodology established in the previous chapter. As the dimensions of the IPMC sample are considered inside α, it is to notice that for the experimental evaluation and solution of the parameters in this work all the samples had the same size. Thus, eq. (15) reflects the proportional tendencies of the displacement at any of the conditions at which the samples were experimentally deformed. Nevertheless, the parameter α may be rearranged to let the material dimensions vary if it is of further interest.

Modeling of the strain and modulus of elasticity

After the solution of eq. (15) for the given parameters, by eq. (3) an expression of strain in terms of the geometry of the strip, the characteristics of the material, and the operational conditions may be obtained.

$$\varepsilon = \alpha \cdot \left(\frac{aX}{ZE}\right) \cdot \left[1 + \left(\frac{V}{V_C}\right)^{-B}\right]^{-1} \tag{16}$$

On the other hand, by relating eq. (3) and eq. (16) it is possible to determine the Modulus of elasticity for the material as a function of the operational and ionic characteristics present in the material.

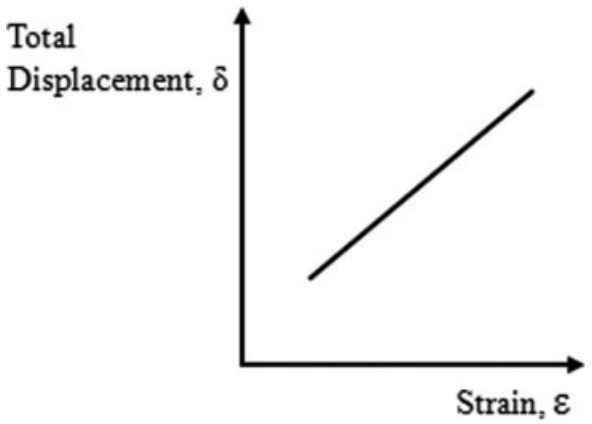

Figure 10 The total displacement as a linear relationship between the factor K and the strain ε.

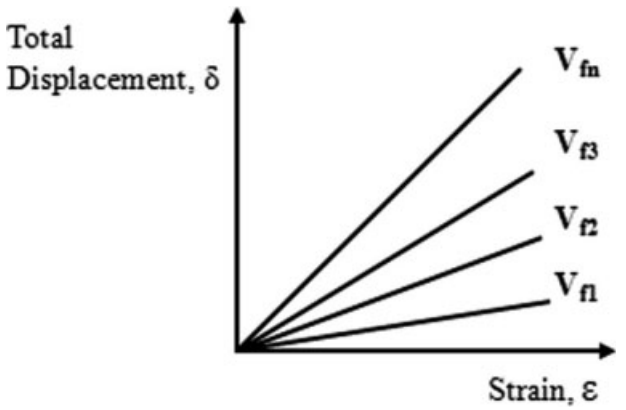

Figure 11 Behavior of total displacement δ versus strain ε at different conditions of potential difference.

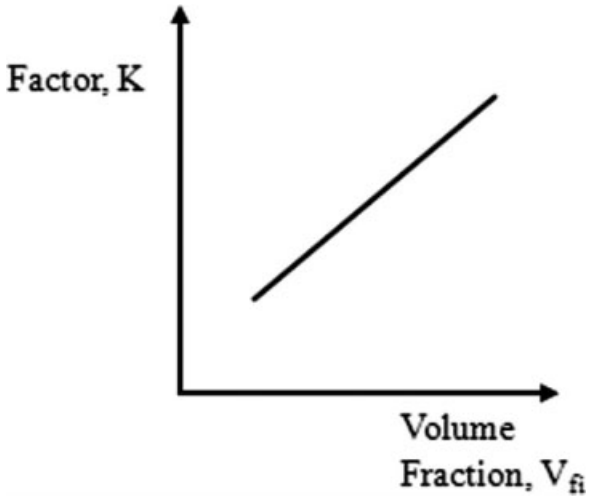

Figure 12 Linear relationship between the factor K and the volume fraction V_{fi}.

$$E = \left(\frac{aXm}{Z}\right) \cdot \left[1 + \left(\frac{V}{V_C}\right)^{-B}\right]^{-1} \quad (17)$$

Equation (17) confirms that the compound material, and particularly of variable composition even under control, possesses also variable mechanical properties; being this one of the most distinctive characteristics of a functional and reconfigurable material. The modulus of elasticity E traditionally is a material constant, however in eq. (17) it is expressed as a function of the factors related to the external and internal changes in the system. In numerical simulation, it may serve the purpose of predicting the changes in the modulus of elasticity due to the change in the conditions given to the material.

RESULTS AND DISCUSSION

Mathematical fitting of the data to obtain parameters

Having eq. (15), a mathematical fitting of the data was obtained defining the parameters for the characteristic voltage V_C and the material parameters α and B. By using Newton-Rahpson method to find the minimum values of the sum of squares of the difference between the calculated and experimental displacements, a mathematical fitting is done for all the five systems, using different values of V_C along the frequency sets, and having the material parameters α and B affecting the over-all system. The results for the constitution of the material system B and the proportionality factor α of the respective ionic species used are presented in Table I. The results for V_C, which represents the potential difference at 50% of transformation, is presented in Table II at different frequency conditions for the respective counter-ions used.

TABLE I
Results for Material Parameters α and B for Respective Counter-Ions Used

Parameter	Counter-ions				
	Li^+	Na^+	K^+	Mg^{2+}	Ca^{2+}
α	56.25	41.85	20.48	41.23	22.52
B	1.64	2.19	3.05	1.87	2.76

TABLE II
Results for Parameter V_C at Different Frequency Conditions with Respective Counter-Ions

Frequency (mHz)	Characteristic potential difference V_C				
	Li^+	Na^+	K^+	Mg^{2+}	Ca^{2+}
50	5.25	4.77	4.31	4.07	2.69
100	5.64	4.98	5.09	4.33	2.89
300	10.76	7.66	7.09	6.53	5.04
500	13.99	9.74	8.16	9.78	6.01
700	16.08	10.78	9.39	10.73	6.55
1000	18.48	19.29	11.29	14.58	8.26
2000	31.77	25.70	14.78	24.10	12.18

Graphical results from the solved equations

The parameters shown in Tables I and II were used in eq. (15) to graph a comparison between the displacements obtain from the model and the experimental data. For illustration purpose, Figures 13–17 shows the results at three different frequency

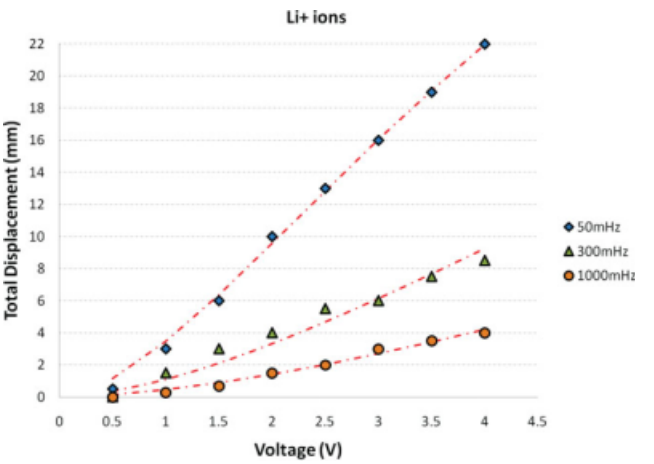

Figure 13 Comparison between the experimental data (marker) and the results obtained from eq. (15) at different frequency values for an IPMC containing Lithium ions. [Color figure can be viewed in the online issue, which is available at www.interscience.wiley.com.]

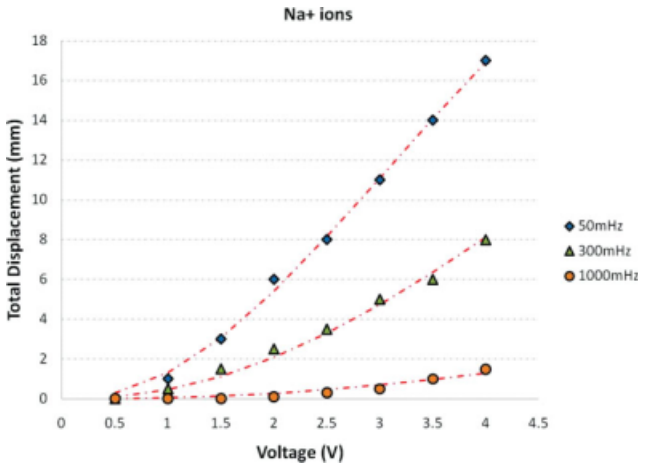

Figure 14 Comparison between the experimental data (marker) and the results obtained from eq. (15) at different frequency values for an IPMC containing Sodium ions. [Color figure can be viewed in the online issue, which is available at www.interscience.wiley.com.]

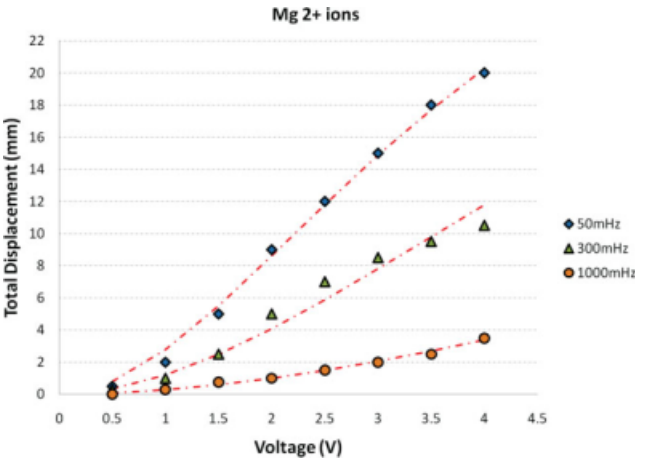

Figure 16 Comparison between the experimental data (marker) and the results obtained from eq. (15) at different frequency values for an IPMC containing Magnesium ions. [Color figure can be viewed in the online issue, which is available at www.interscience.wiley.com.]

conditions. The dash line represents the model results, while the markers represent the experimental data.

Lithium has an ionic radius of 76 pm,[22] which makes it one of the smallest ions used. The basic tendency of Lithium is the same as the rest of the ionic species to explain further on. As there is an increase in the voltage, the displacement of the IPMC strip also increases. However, as the values of frequency increase, the displacement values decrease significantly. Further on, it is noticed how the ion contents affects this values, as the other cations were compared.

In the case of sodium, its ions have a radius of 102 pm[22]; which is near the size of potassium. This make the sodium ions the second largest of the cationic species used. The results in this case show less performance in the displacement making it lower than the case of lithium but still later seen to be larger than potassium when used as the ion content of the IPMC.

Potassium ions have a radius of 138 pm[22] and are the largest of the five species used. As it is to be seen, this ion content is the one which gave the smallest values for the total displacement. The tendencies to increase the displacement at the increase of the voltage and the decrease of the frequency remain The results indicate that the potassium has almost half the performance of lithium ions when achieving the deformation, although potassium is a

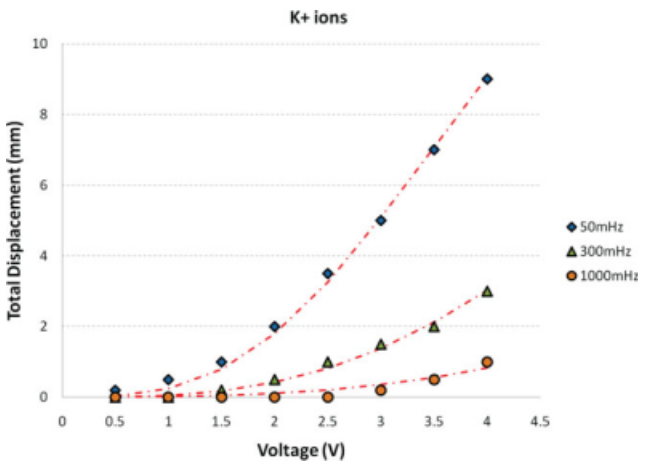

Figure 15 Comparison between the experimental data (marker) and the results obtained from eq. (15) at different frequency values for an IPMC containing Potassium ions. [Color figure can be viewed in the online issue, which is available at www.interscience.wiley.com.]

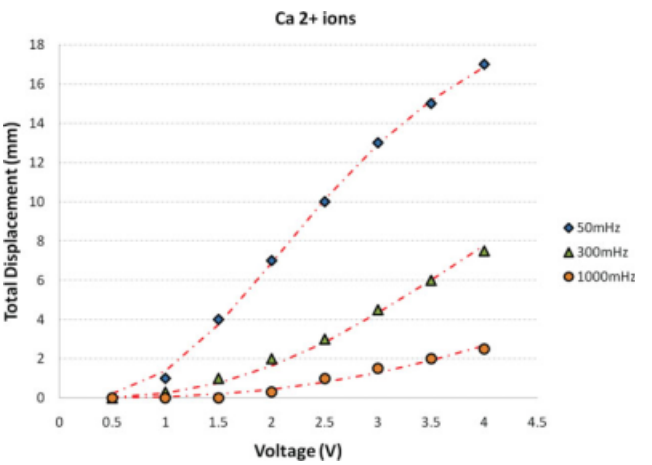

Figure 17 Comparison between the experimental data (marker) and the results obtained from eq. (15) at different frequency values for an IPMC containing Calcium ions. [Color figure can be viewed in the online issue, which is available at www.interscience.wiley.com.]

larger cation and should occupy more volume. However, it is considered that potassium may travel much slower than Lithium due to its size. Larger cationic species seem to have more difficulties to travel along the Nafion polymer back-bone chains; so it is considered that not all the potassium tend to reach the cathode side.[23] Having ions still scattered at the center of the cross section instead of the expanding side may result in lower displacements as shown in the graphed in Figure 15.

Magnesium has an ionic radius of 72 pm[22]; placing it as the smallest cation used in the experimentation, and is also a divalent cationic specie. As it is mentioned before, divalent cations have a greater tendency to orient and polarize water molecules and to resist dehydration.[24] Any change in the tendency based on the valence of the cation, besides the ionic radius, is of interest for the analysis of the displacement obtained from the IPMC. If the results from the monovalent species sustained a tendency at which the smallest cation, the lithium, showed the greatest displacements, when comparing the lithium and magnesium the results show something different. Although the results are very similar to the lithium, the performance of magnesium is slightly lower.

Calcium is also a divalent cation specie as the Magnesium. It has an ionic radius of 99 pm,[22] which is compared to the sodium of 102 pm. The results showed a slightly better performance than those seen when using Sodium as ionic content; especially at higher frequencies with values of 1000 and 200 mHz where in the case of Sodium the response is lesser. Figure 17 presents the results obtained from experimentation. Based on the other results, the tendency regarding the type of cationic specie seems to indicate that the total displacement increases with the decrease of the ionic radius of the cation inside the IPMC strip. This information is useful for further modeling of the bending action of the IPMC.

All five species have been considered small ions that achieve a fast response in the IPMC.[23] As we have presented, the effect of the counter-ion in the response of the IPMC depended on the movement of these cationic ion species in the swelling film along with water due to the migration of both into the cathode side. However, there different sizes and charge values, which seemed to affect the response in such a way from one cation to another.

CONCLUSION

A constitutive model for the bending deformation of an electrically induced IPMC was proposed, developed, and solved using experimental data. The constitutive equation was result of combining the bending deformation of a beam system that is subject to a (virtual) load, which is then account as the result of an analogical phase transformation which forms two phases at both sides of the cross section of the IPMC samples. A phase transformation model was adjusted to represent the internal changes in the volume fraction of the contained counter-ions inside the polymer as a function of the applied voltage V, a related to a characteristic voltage V_C which depends on the frequency conditions, and a parameter B which is a function of the inner constitution of the material base on the ionic content. The parameters needed for the model were defined using a mathematical fitting by minimum sum of squares, and solving by the Newton-Rhapson method. The dimensions of the IPMC samples for the experimental evaluation were always the same leaving the parameters solved in this work to reflect the proportional tendencies of the displacement at any of the conditions at which the samples were experimentally deformed. Nevertheless, the parameter α may be rearranged to let the material dimensions vary for further use; as it may be possible to calculate other properties as strain and modulus of modulus of elasticity for design purposes.

The experimental data compared to the results from the model show an acceptable fitting for most of the systems; demonstrating the effectiveness of the model in the proposed approach using the phase transformation theory. The constitutive model solved here, may be use as an engineering tool for quick reference of the relation between the bending action of the IPMC and the electrical input required to trigger its electroactive phenomenon. This tool may be further use for design and simulation of IPMC systems regarding the active positioning of the polymer strip based on the requirements of the engineers and designers without the necessity of a deep chemical or materials background.

References

1. Oguro, K.; Kawami, Y.; Takenaka, H. Trans J Micromachine Soc 1992, 5, 27.
2. Shahinpoor, M. Smart Mater Struct 1992, 1, 91.
3. Sadeghipour, K.; Salomon, R.; Neogi, S. Smart Mater Struct 1992, 1, 172.
4. Shahinpoor, M.; Kwang, J. K. Smart Mater Struct 2001, 10, 819.
5. Kwang, J. K.; Shahinpoor, M. Smart Mater Struct 2003, 12, 65.
6. Shahinpoor, M.; Kwang, J. K. Smart Mater Struct 2004, 13, 1362.
7. Bar-Cohen, Y. In Proceedings of the 42nd AIAA Structural Dynamics, and Materials Conference (SDM), Gossamer Spacecraft Forum (GSF), Seattle WA, USA, 2001.
8. Shahinpoor, M. Int J Adv Robotic Syst 2005, 2, 161.
9. de Gennes, P. G.; Okumura, K.; Shahinpoor, M.; Kim, K. J. Europhys Lett 2000, 50, 513.
10. Asaka, K.; Oguro, K. J Electroanal Chem 2000, 480, 186.
11. Nemat-Nasser, S.; Li, J. Y. J Appl Phys 2000, 87, 3321.

12. Nemat-Nasser, S. J Appl Phys 2002, 92, 2899.
13. Nemat-Nasser, S.; Wu, Y. J Appl Phys 2003, 93, 5255.
14. Tadokoro, S. In Proceedings of IEEE; ICRA: San Francisco, California, 2000; p 1340.
15. Tadokoro, S.; Yamagami, S.; Takamori, T.; Oguro, K. In Proceedings of the SPIE; SPIE Publication 3987: San Jose, California, 2000; p 92. 3987
16. Tadokoro, S.; Takamori, T.; Oguro, K. In Proceedings of the SPIE; SPIE Publication 4329: Bellingham, Washington, 2001; p 28.
17. Oguro, K. World Wide Electroactive Polymer Actuators Webhub. Available at: http://ndeaa.jpl.nasa.gov/nasa-nde/lommas/eap/IPMC_PrepProcedure.htm. Accessed on October 2008.
18. Cortes, J. A. Ph.D. Thesis, Hiroshima University: Hiroshima, Japan, 1993.
19. Tsuta, T.; Cortes, J. A. In Proceedings of the 4th ICTP Numerical Analysis/FEM/Experimental Analysis/Forming Property/Extrusion: Beijing, China, 1993; p 564.
20. Cortes, J. A.; Tsuta, T.; Iwamoto, T. In Proceedings of the Conference on Computational Engineering and Science: Japan, 2000; p 719.
21. Cortes, J. A.; de la Garza, R.; Gallegos, S.; Florez, L.; Martínez, M. Mater Manuf Process 2007, 22, 318.
22. Shanon, R. D. Acta Crystallogr Sect A 1976, 32, 751.
23. Bao, X.; Bar-Cohen, Y.; Lih, S. Presented at the Smart Structures and Mater Symposium, Paper 4695–27: San Diego, California, 2002.
24. Woods, K. K.; McFail-Isom, L.; Sines, C. C.; Howerton, S. B.; Stephens, R. K.; Williams, L. D. J Am Chem Soc 2000, 7, 1546.